Available online at www.sciencedirect.com
ScienceDirect
Journal of Solid State Chemistry 180 (2007) 2346–2355
JOURNAL OF SOLID STATE CHEMISTRY
www.elsevier.com/locate/jssc

The chemistry of the phosphates of barium and tetravalent cations in the 1:1 stoichiometry

Karin Popa[a,b,*], Damien Bregiroux[a,c], Rudy J.M. Konings[a], Thomas Gouder[a], Aurelian F. Popa[d], Thorsten Geisler[e], Philippe E. Raison[a]

[a]European Commission, Joint Research Centre, Institute for Transuranium Elements, P.O. Box 2340, 76125 Karlsruhe, Germany
[b]"Al.I. Cuza" University, Department of Inorganic and Analytical Chemistry, 11-Carol I Blvd., 700506 Iasi, Romania
[c]Université Pierre et Marie Curie-Paris 6, CNRS UMR 7574, Chimie de la Matière Condensée de Paris, 4 Place Jussieu Paris, F-75005, France
[d]Faculté des Sciences-Université de Nantes, Institut des Matériaux Jean Rouxel-Laboratoire de Chimie des Solides, B.P. 32229, 44322 Nantes Cedex 3, France
[e]Institut für Mineralogie, Westfälische Wilhelms-Universiät, Corrensstr., 24, 48149 Münster, Germany

Received 11 April 2007; received in revised form 8 June 2007; accepted 10 June 2007
Available online 15 June 2007

Abstract

The chemistry of phosphates of barium and tetravalent cations [$BaM^{IV}(PO_4)_2$] is reviewed. Such phosphates crystallise in the $C2/m$ space group for M^{IV} = Ti, Zr, Hf, Ge, Sn, and Mo, and in the $P2_1/n$ space group for $BaTh(PO_4)_2$. The existence of $BaM^{IV}(PO_4)_2$ in which M^{IV} = Pb, Ce, and U is further evaluated. Several aspects, such as phase transitions in the compounds with yavapaiite structure, solid solutions of $BaM^{IV}(PO_4)_2$ compounds and practical applications are briefly discussed.

Keywords: Barium; Ceramics; Conditioning; Crystal structure; Phosphates; Tetravalent cations; Phase transition

1. Introduction

The chemistry and the crystal structure of phosphates containing tetravalent cations have recently been reviewed by Brandel and Dacheux [1,2]. These authors have discussed the relatively high numbers of phosphate compounds that have been synthesised and characterised during the last two decades. They also re-analysed the chemistry and crystal structure of some previously wrongly identified compounds, containing Th, U, and Np. Moreover, they proposed a new phosphate systematics and discuss the implications for the immobilisation of tetravalent actinides in these compounds.

According to the new Brandel and Dacheux systematics all the phosphates can be classified on the basis of the general framework $[(M^h)_m(A^q)_p]^k$ where $k = hm+pq$. Applied to tetravalent M^{IV} cations (M^{IV} = Si, Sn, Pb, Ti, Zr, Hf, Re, Mo, Ce, Th, Pa, U, Np, and Pu) the various phosphate anions (A^q) could be $H_2PO_4^-$, HPO_4^{2-}, PO_4^{3-}, $P_2O_7^{4-}$, PO_3^-, etc. Three main families result from this formula: uncharged compounds ($k = 0$), phosphates with cationic framework ($k>0$) and with anionic framework ($k<0$).

$BaM^{IV}(PO_4)_2$ compounds are part of the sub-group of phosphates of the $(M^n)_xM(PO_4)_2$ type ($q = -3$ and $m = 1$, anionic framework), in which M^n is Ba^{2+} and $x = 1$. Such phosphates can be considered as derivatives of hydro phosphates $M^{IV}(HPO_4)_2$, where Ba^{2+} replaces both protons.

$BaM^{IV}(PO_4)_2$ phosphates are interesting materials as catalysts, ion exchangers, ionic conductors and luminescence materials. $BaZr(PO_4)_2$ and $BaHf(PO_4)_2$ are used in medical imaging with the aim of reducing the exposure of the patient to X-rays while maintaining the structural features of the X-ray image. Such phosphates fulfil the requirements for an "intensifier screen". They show: (i) good X-ray absorption

*Corresponding author. "Al.I. Cuza" University, Department of Inorganic and Analytical Chemistry, 11-Carol I Blvd., 700506 Iasi, Romania. Fax: +49 7247 99670.
E-mail addresses: karin.popa@ec.europa.eu, kpopa@uaic.ro (K. Popa).

0022-4596/$ - see front matter © 2007 Elsevier Inc. All rights reserved.
doi:10.1016/j.jssc.2007.06.006

in the diagnostic medical energy range (15–100 keV), (ii) high luminescence efficiency, (iii) emission in the green to near-UV region, (iv) proper crystallite size and shape, (v) air and water stability, and (vi) relatively easy large-scale production. Finally, compounds of this group are potential candidates for the immobilisation of high-level nuclear waste, which is the background of the present research.

In the review of Brandel and Dacheux, only $BaTh(PO_4)_2$ (as reported in [3]), $BaU(PO_4)_2$ [4], and $BaZr(PO_4)_2$ are mentioned. Nevertheless, searching for published studies on end members of solid solutions of the form $(Ln,An)^{III}_{2-2x}M^{II}_xM^{IV}_x(PO_4)_2$ with *Ln* and *An* representing lanthanides and actinides, respectively, we found several other studies which reported the existence of $BaM^{IV}(PO_4)_2$ compounds with M^{IV} = Ti, Hf, Ge, Sn, Mo, and Ce as well as solid solutions of such compounds containing Zr, Hf, and Ce. However, we did not find any study on compounds containing Re, Pb, Pu, and Np. This was the incentive to start a systematic study on $BaM^{IV}(PO_4)_2$ compounds. The literature survey and our newest experimental data are summarised in the present research review.

2. Synthesis

During the last 100 years, several methods of synthesis were employed to obtain compounds with the general formula $BaM^{IV}(PO_4)_2$. These are solid-state reaction, hydrothermal syntheses, sol–gel reactions and even single-crystal growth from a flux.

Masse and Durif [5] obtained $BaM^{IV}(PO_4)_2$ (M^{IV} = Ge, Ti, Zr, and Sn) by a solid-state reaction. Equimolar quantities of $BaCO_3$, $M^{IV}O_2$, and $(NH_4)_2HPO_4$ were ground together and slowly heated to 300 °C for 24 h, mixed again, and then heated to 1100 °C for several days. The same compounds as well as the one with Hf were obtained by Paques-Ledent [6] in platinum or corundum crucibles, using the procedure described in [5]. The general chemical reaction is

$$BaCO_3 + M^{IV}O_2 + 2(NH_4)_2HPO_4 \rightarrow BaM^{IV}(PO_4)_2 + 4NH_3 + CO_2 + 3H_2O.$$

$BaZr(PO_4)_2$ was also obtained by Fukuda et al. [7] using a two-step procedure as follows. A mixture of stoichiometric amounts of reagent-grade $BaCO_3$ and ZrO_2 were firstly heated in air at 1500 °C, resulting in the formation of $BaZrO_3$. This double oxide was than mixed with $NH_4H_2PO_4$ (equimolar quantities), pressed into pellets, and reacted at 1200 °C. We also obtained this compound in a single step by reacting $BaCO_3$ and ZrO_2 (equimolar quantities) and $(NH_4)_2HPO_4$ (25% excess) in an alumina crucible for 100 h at 1200 °C [8]. For shorter reaction times or lower temperatures, ZrO_2, ZrP_2O_7, or even $Ba_3(PO_4)_2$ were detected as additional phases. Studying the systems $M^{II}O$:ZrO_2:P_2O_5, Petkov and Orlova [9] obtained a pure phase of $BaZr(PO_4)_2$ from equimolar quantities of BaO, ZrO_2, and P_2O_5 at 1000 °C.

We also obtained $BaM^{IV}(PO_4)_2$ compounds with M^{IV} = Ti, Ge, Sn, and Hf by solid-state reactions [10,11]. In this case, $BaCO_3$, $M^{IV}O_2$ (equimolar quantities), and $(NH_4)_2HPO_4$ (0–25% excess) were heated in an alumina crucible in air at 1200–1250 °C for 100–200 h. For these compounds, the solid-state reaction was followed by differential thermal analysis (DTA). Only the events occurring between 750 and 1000 °C are presented in Fig. 1.

All the peaks observed before 600 °C reflect the fusion and decomposition of the phosphate precursor $(NH_4)_2HPO_4$ and the decarbonation of $BaCO_3$ and are not shown in Fig. 1. For all five compounds, an endothermic peak close to 870 °C was detected (marked with a star), that could correspond to the fusion of a barium phosphate, probably $Ba(PO_3)_2$. $Ba(PO_3)_2$ melts at 877 °C according to the phase diagram given by McCauley and Hummel [12]. This gives evidence that BaO first reacts with the phosphate precursor to form $Ba(PO_3)_2$ (note that in the starting mixture, Ba/P ratio is 1/2). For example, the XRD pattern of a mixture of $BaCO_3$:ZrO_2:$(NH_4)_2HPO_4$ = 1:1:2 heated at 800 °C indicates the presence of the following crystalline compounds: ZrO_2, $Zr_2P_2O_7$, $Ba(PO_3)_2$, $Ba_3(P_2O_7)(PO_3)_2$, and $Ba_2P_2O_7$. The latest three phosphates present different Ba:P ratios: 1.0, 0.75, and 0.5, respectively. $Ba_3(P_2O_7)(PO_3)_2$ appears as an intermediate compound. The incorporation of Zr(IV) into the final compound takes place at higher temperatures.

$BaMo(PO_4)_2$ was synthesised both as polycrystalline powder and single crystals by Leclaire et al. [13]. The reaction to prepare pure powder of $BaMo(PO_4)_2$ was carried out at 800 °C for 12 h, quenching the sample at room temperature. The growth of single crystals was performed in two steps. In the first step, a mixture of $BaCO_3$, MoO_3, and $(NH_4)_2HPO_4$ with a nominal composition of $Ba_3Mo_4P_6O_{24}$ was heated at 700 °C to obtain a dry mixture of oxides. In a second step, the appropriate amount of Mo (1 mole) was added. The ground mixture

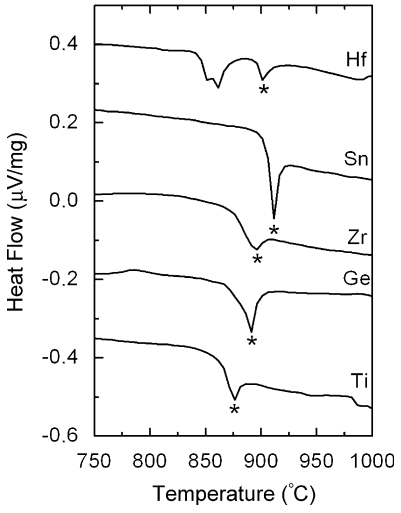

Fig. 1. The DTA curves for the starting products $M^{IV}O_2 + BaCO_3 + 2(NH_4)_2HPO_4$.

was then sealed in an evacuated quartz ampoule, annealed for 12 h at 900 °C and then quenched to room temperature.

Orlova et al. [14] reported the synthesis of impure "$BaCe(PO_4)_2$" by reacting phosphoric acid, $(NH_4)_2Ce(NO_3)_6$, and barium chloride or nitrate. This mixture forms a gel that was successively tempered at temperatures of 600, 800, and 1100 °C for 20–24 h at each temperature with intermediate grinding.

$BaTh(PO_4)_2$ has successfully been synthesised by an all-gel method [3] derived from a procedure that has been proposed by Luth and Ingamels [15]. Stoichiometrical amounts of thorium nitrate and barium carbonate were gellified by addition of $(NH_4)_2HPO_4$ solution and the gel was rinsed, dried, and finally tempered [3]. Pure compounds were obtained using two different annealing conditions: (1) at 1 bar at 1200 °C for 24 h and (2) at 2500 bar at 700 °C for 7 days. Brandel et al. [16] reported a compound corresponding to the Ba:Th:P = 1:1:2 stoichiometry at 1100 °C and autogenic pressure. Our solid-state trials starting from $BaCO_3$, ThO_2 and $(NH_4)_2HPO_4$ in equimolar quantities, which were sintered in an alumina crucible at 1300 °C for 100 h under a nitrogen atmosphere led to the same compound previously reported by Brandel et al. [16]. This compound is different from the monoclinic $M^{II}Th(PO_4)_2$ brabantite-like compounds, monoclinic $BaM^{IV}(PO_4)_2$ (M^{IV} = Ti, Zr, Hf, Ge, Sn) yavapaiite-like compounds, as well as the cubic $Ba_7Th(PO_4)_6$ [24].

Tananev [4] reported the existence of $BaU(PO_4)_2$ as described by Colani [17]. For the synthesis of this compound U(IV) phosphate was sintered with $BaCl_2$ to obtain a compound that corresponds to the stoichiometry Ba:U:P = 1:1:2. Any further characterisation of the final compound has not been carried out and, to our knowledge, no further trials to synthesise this compound have been published to date. Even the existence of the starting compound $U_3(PO_4)_4$ is doubtful [18–20]. We note here that all our attempts to obtain $BaU(PO_4)_2$ has led to a mixture of crystalline products in which UP_2O_7 is the main phase.

Finally, we would like to mention that other phosphates, containing barium and tetravalent cations like $Ba_{0.5}Ti_2(PO_4)_3$ [21], $Ba_{0.5}Zr_2(PO_4)_3$ [22], and $Ba_7Th(PO_4)_6$ [23] have successfully been synthesised and characterised, but these compounds are not of interest here as they do not correspond to the 1:1 stoichiometry.

3. Crystal structure

The known $BaM^{IV}(PO_4)_2$ compounds generally crystallise in two monoclinic space groups, as presented in Table 1.

Compounds with M^{IV} = Ti, Zr, Hf, Ge, Sn, and Mo crystallise in the monoclinic $C2/m$ space group and their crystal structure resembles that of the mineral yavapaiite, $KFe(SO_4)_2$, for which the structure was refined by Graeber and Rosenzweig [26] using single-crystal X-ray diffraction (XRD) data. The yavapaiite structure is a layered structure that exhibits close relationship with the

Table 1
Crystal data of $BaM^{IV}(PO_4)_2$ compounds at room temperature

M^{IV}	$r(M^{IV})$[a] [25]	Space group	a (Å)	b (Å)	c (Å)	β (deg.)	V (Å^3)	Reference
Ge	0.53	$C2/m$	8.074	5.298	7.750	95.24	330.1	Paque-Ledent [6]
			7.952	5.066	7.700	94.94	309.0	Masse and Durif [5]
			7.9864	5.0733	7.7111	94.77	311.4	Popa et al. [11]
Ti	0.605	$C2/m$	8.250	5.176	7.713	94.18	328.5	Paque-Ledent [6]
			8.250	5.176	7.713	94.18	328.4	Masse and Durif [5]
			8.2677	5.1841	7.7291	94.14	330.4	This study
Mo	0.65	$C2/m$	8.211	5.2757	7.816	94.77	337.4	Leclaire et al. [13]
Sn	0.69	$C2/m$	8.200	5.230	7.870	94.50	336.4	Masse and Durif [5]
			8.2079	5.2394	7.8846	94.52	338.0	This study
Hf	0.71	$C2/m$	8.525	5.284	7.874	93.12	354.2	Paque-Ledent [6]
			8.550	5.296	7.883	93.13	356.4	Keller and McCarthy [24]
			8.5389	5.2928	7.8811	93.17	355.6	Popa et al. [10]
Zr	0.72	$C2/m$	8.531	5.293	7.875	93.08	355.0	Masse and Durif [5]
			8.531	5.293	7.873	93.08	355.1	Paque-Ledent [6]
			8.5629	5.3082	7.8956	93.06	358.3	Fukuda et al. [7]
			8.5706	5.3032	7.8868	92.99	357.9	Popa et al. [8]
Ce[b]	1.02	$P2_1/n$	*6.776*	*7.016*	*6.437*	*103.42*	*297.6*	Orlova et al. [14]
			6.800	*7.027*	*6.475*	*103.46*	*300.9*	This study
Th	1.09	$P2_1/n$	6.944	7.161	6.670	102.88	323.3	Montel et al. [3]
			6.950	7.162	6.675	102.88	323.9	Montel et al. [3]

[a]The coordination number is considered [IX for Ce(IV) and Th(IV) and VIII for others M(IV)].
[b]The "$BaCe(PO_4)_2$" compound does not exist, as discussed later in this paper.

three-dimensional framework of β-cristobalite, α-$NaTiP_2O_7$, and $CsMoOP_2O_7$ [13].

The crystal structure of $BaZr(PO_4)_2$ was refined using Fukuda et al. [7] by conventional X-ray powder diffraction by direct methods and further refined via a profile matching mode.

A similar refinement procedure was used in this study for $BaHf(PO_4)_2$ (Fig. 2). The refined cell parameters were $a = 8.53892\ (18)$ Å, $b = 5.29277\ (12)$ Å, $c = 7.88106\ (19)$ Å and $\beta = 93.1702\ (16)^\circ$ and the volume $V = 355.636\ (14)$ Å^3. Final reliability indices were $R_w = 0.0470$, $R = 0.0348$, and $R_B = 0.0457$ ($\chi^2 = 0.0345$) with an electronic residue of $\Delta\rho_{max} = 0.58$ e Å^{-3} and $\Delta\rho_{min} = -0.57$ e Å^{-3}.

The crystal structure consists of BaO_{10}, HfO_6, and PO_4 units. The PO_4 and the BaO_{10} polyhedra share edges, containing the two oxygen atoms O2 and O3, and corners (O2 atoms) to produce two-dimensional sheets. These sheets are stacked along the c direction and are connected by means of O2 atoms to the HfO_6 octahedra (Fig. 3). Each

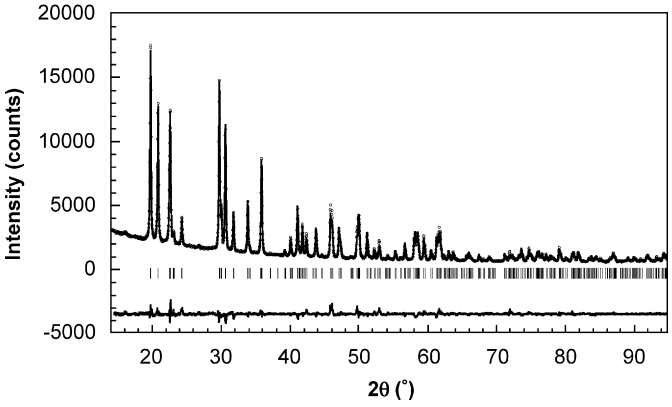

Fig. 2. Room-temperature Rietveld refinement plot of $BaHf(PO_4)_2$, showing the observed (o), calculated (solid line), and difference pattern (lower). The vertical marks indicate the positions of allowed Bragg reflections.

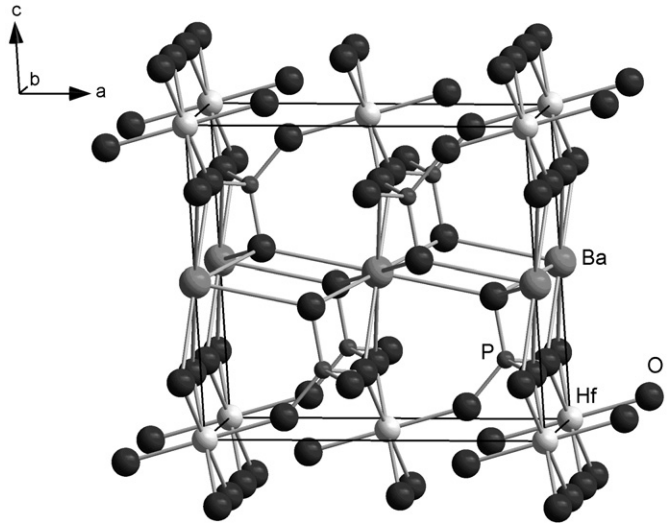

Fig. 3. Crystal structure of $BaHf(PO_4)_2$ at room temperature.

of the BaO_{10} polyhedra shares one edge with one HfO_6 unit located below and above the sheet. Each PO_4 is connected via three corners with HfO_6 polyhedra from the same side of the sheet, i.e., the PO_4 groups that are located at $z < 0.5$ and $z > 0.5$ are connected below and above the sheet, respectively (Table 2).

In the HfO_6 octahedra (Fig. 4) there are four identical, shorter, Hf–O3 bonds (Table 3) and two other, slightly longer bonds (Hf–O1). All the O1–Hf–O3 angles are close to 90°, only the O3–Hf–O3 angle is far from the value of 90°. The PO_4 tetrahedra are more distorted, with the P–O bonds taking three different values according to the type of oxygen atoms O1, O2, and O3, respectively.

From Fig. 5 it is evident that all compounds containing a tetravalent cation with an ionic radius smaller than 0.72 Å for a coordination of VI crystallise in the monoclinic $C2/m$ space group as they define a good linear correlation between the ionic radius and the unit-cell volume. Using this linear correlation, the volume of the $BaRe(PO_4)_2$ compound can be extrapolated to be 334 Å^3. Nevertheless, there are no reports about the existence of such a phosphate in the literature. We therefore tried to synthesise this compound by conventional solid-state reaction under

Table 2
Atomic positions in $BaHf(PO_4)_2$ compound

Atom	x	y	z	U_{eq}
Hf	0.00000	0.00000	0.00000	0.009 (2)
Ba	0.00000	0.00000	1/2	0.021 (3)
P	0.3597 (8)	0.00000	0.2240 (8)	0.024 (5)
O1	0.237 (2)	0.00000	0.0731 (19)	0.079 (12)
O2	0.3370 (19)	0.00000	0.4259 (15)	0.077 (14)
O3	0.4577 (7)	0.2705 (16)	0.1965 (10)	−0.003 (7)

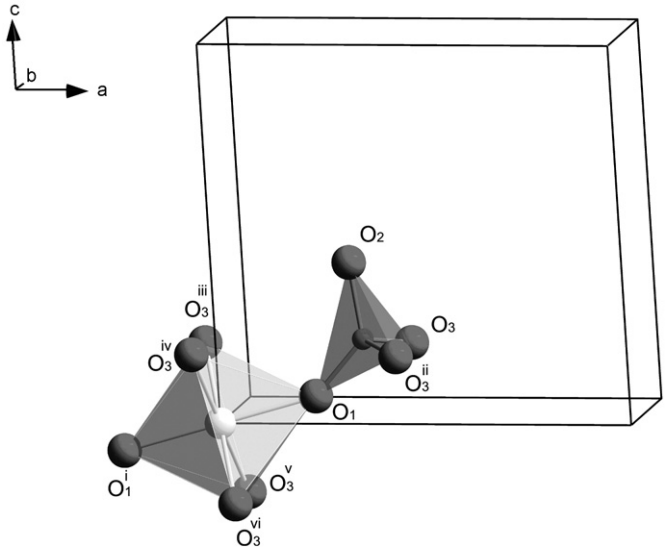

Fig. 4. Arrangement of the HfO_6 octahedron and PO_4 tetrahedron in the unit cell of $BaHf(PO_4)_2$. Symmetry codes: (i) $-x, y, -z$, (ii) $x, -y, z$, (iii) $-0.5+x, 0.5-y, z$, (iv) $-0.5+x, -0.5+y, z$, (v) $0.5-x, 0.5-y, -z$, (vi) $0.5-x, -0.5+y, -z$.

Table 3
Selected geometric parameters for BaHf(PO4)2 (Å, °)

Hf–O_1, Hf–O_1^{I}	2.073(17)	O_1^{i}–Hf–O_3^{iii}, O_1^{i}–Hf–O_3^{iv}	89.98(20)
		O_1–Hf–O_3^{v}, O_1–Hf–O_3^{vi}	
Hf–O_3^{iii}, Hf–O_3^{iv}	2.016(9)	O_1^{i}–Hf–O_3^{v}, O_1^{i}–Hf–O_3^{vi}	90.03(20)
Hf–O_3^{v}, Hf–O_3^{vi}		O_1–Hf–O_3^{iii}, O_1–Hf–O_3^{iv}	
		O_3^{iii}–Hf–O_3^{iv}, O_3^{v}–Hf–O_3^{vi}	74.1(3)
		O_3^{iii}–Hf–O_3^{v}, O_3^{iv}–Hf–O_3^{vi}	105.9(3)

Symmetry codes: (i) $-x$, y, $-z$, (ii) x, $-y$, z, (iii) $-0.5+x$, $0.5-y$, z, (iv) $-0.5+x$, $-0.5+y$, z, (v) $0.5-x$, $0.5-y$, $-z$, (vi) $0.5-x$, $-0.5+y$, $-z$.

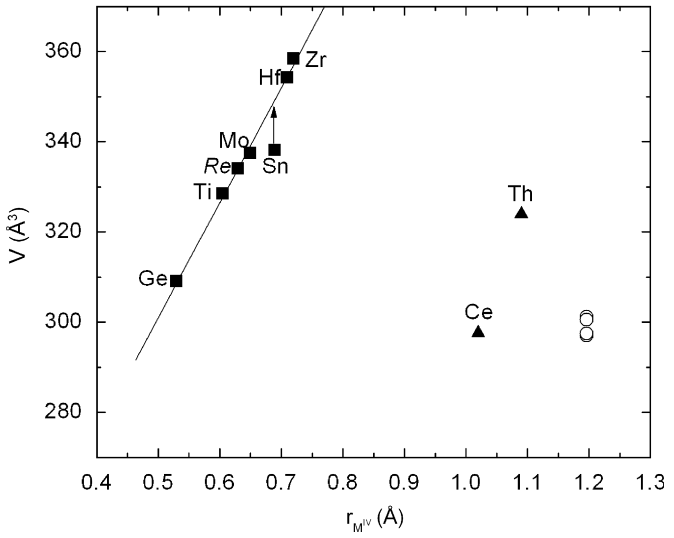

Fig. 5. Variation of the unit-cell volume of $BaM^{IV}(PO_4)_2$ as a function of the ionic radii [25] of M^{IV} cations. The points correspond to the result of our study, except for M^{IV} = Mo [13] and Th [3]. For the rhenium compound, the value was calculated by linear regression. The open circles represent $CePO_4$, reported by different authors [27–30].

argon or nitrogen atmosphere or in quartz tube under vacuum. The experimental products were always polyphase compounds. The main problem seems to be the fact that at temperatures between 1000 and 1200 °C rhenium gets vaporised, which resulted in a shift of the Ba–Re ratio smaller than 1 during the sintering step. The problem remains even if we start with an excess of Re^{IV} (up to 50%).

Our attempts to synthesise $BaPb(PO_4)_2$ was also not satisfactory, although identical synthesis conditions have been applied. The final compound has optically a glassy appearance. XRD measurements revealed that the product is amorphous or microcrystalline. A first indication of the reaction between the starting compounds is a colour change from black to white. It is noteworthy that this compound is missing in previous systematic studies on such kind of phosphates [5,6]. Scanning electron microscopy (SEM) investigations and energy-dispersive X-ray (EDX) analyses of the glass indicated that it is a single phase (on micrometre scale) having a molar ratio of Ba:Pb:P = 1:1:2 that agrees with that of the hypothetical $BaPb(PO_4)_2$ compound. The preferential formation of a lead phosphate glass is expected since Pb oxide acts as flux that dramatically reduces the melting point of the system.

The synthesis of "$BaCe(PO_4)_2$" was reported as part of an extensive research on phosphates of Ce(IV) with Li, Na, K, Rb, Cs, Mg, Ca, Sr, Ba, and Cd by Orlova et al. [14]. According the Rietveld refinement data, "$BaCe(PO_4)_2$" should belong to the $P2_1/n$ with the lattice parameters listed in Table 1. The authors have not performed any other characterisation of this compound.

Our own attempts to synthesise this phosphate by solid-state reaction or precipitation methods, as described in [14] and in the synthesis chapter of this work, resulted in a green product. Independent of the synthesis method, the powder XRD pattern of this material is compatible with the $P2_1/n$ space group, but the Rietveld refinement proved that the pattern is perfectly explained by $CePO_4$, with monazite structure (Fig. 6). Moreover, the curvature of the base line between 20° and 32° 2θ corresponds to the signature of an amorphous phase that should contain the barium.

SEM investigation on the product clearly indicates that it is a mixture of two phases (Fig. 7): (i) well-defined single crystals with a chemical composition Ba:Ce:P:O = 0:1:1:4, and (ii) a glassy phase with a (Ba + Ce):P:O ratio of 1:2:7.

The thermal analysis of the $BaCO_3$–CeO_2–$(NH_4)_2HPO_4$ mixture also provides a very clear information about the cerium behaviour during heating. The weight loss visible between 700 and 1000 °C in thermogravimetric curve shown in Fig. 8 can be attributed to the reduction of Ce(IV) in Ce(III) with O_2 release. Moreover, this reduction seems to be complete since the observed weight loss is very close to the theoretical one (0.8% and 0.7%, respectively). We can also note that this reduction occurs at a temperature that corresponds to the melting point of

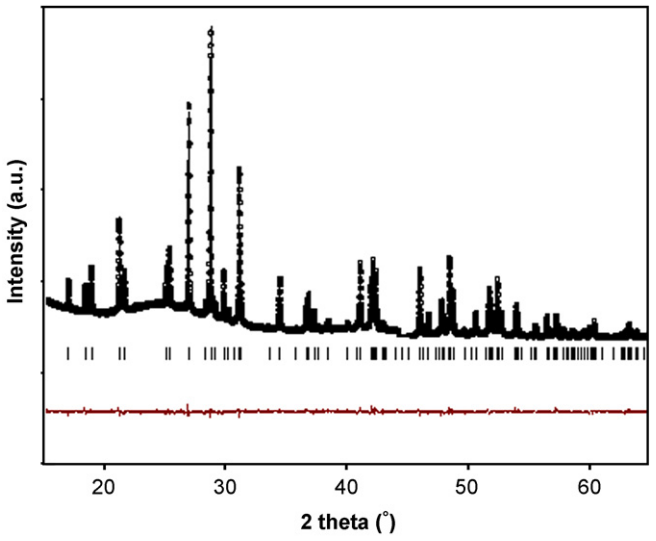

Fig. 6. Comparison between observed (o) and calculated (upper solid line) XRD patterns of "$BaCe(PO_4)_2$". The difference curve is shown in the lower part of the figure. Vertical marks indicate the positions of possible Bragg reflections.

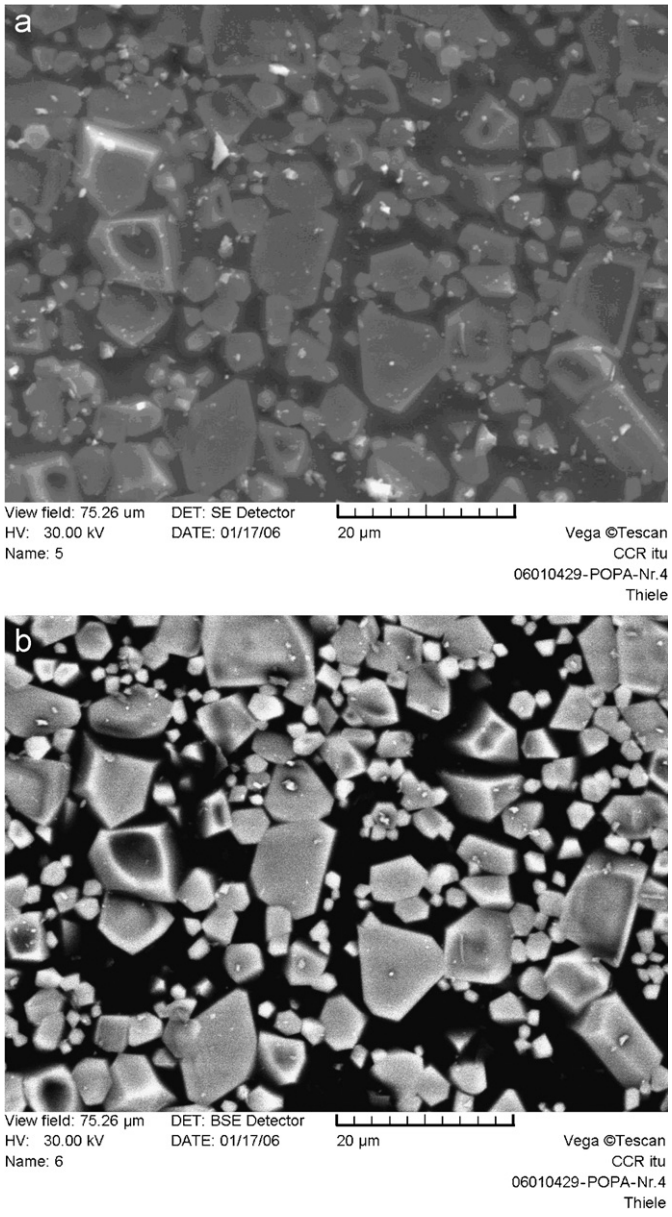

Fig. 7. Secondary electron (SE) and backscattered electron (BSE) images of "$BaCe(PO_4)_2$".

$Ba(PO_3)_2$, as also observed for other phosphates with different M site elements (see Fig. 1).

In addition, the Raman spectrum of the "$BaCe(PO_4)_2$" compound shows the fundamental bands of $CePO_4$ and two broad bands that overlap with bands resulting from crystalline BaO in the mixture. Furthermore, the colour and the appearance of the final compound clearly indicate the formation of $CePO_4$ with a monazite structure, which explains the excellent refinement into the $P2_1/n$ space group. Note that the unit-cell volume of "$BaCe(PO_4)_2$" (Fig. 5) as obtained in [14] and by us is equal or slightly smaller than that of $CePO_4$ [27–30].

To determine whether Ce is in the oxidation state III or IV, a sample of nominal "$BaCe(PO_4)_2$" composition was analysed by X-ray photoemission spectroscopy (XPS). The

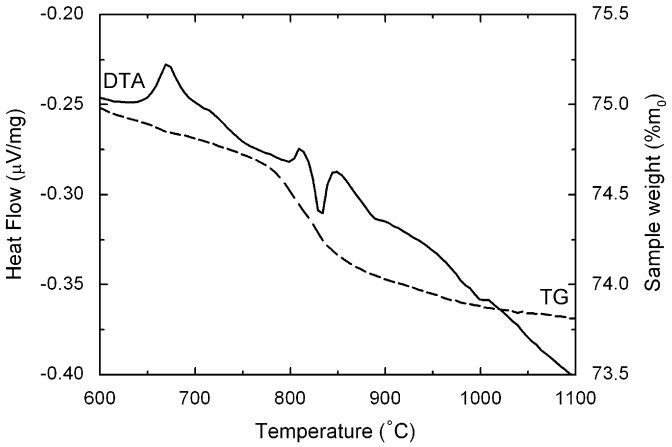

Fig. 8. The TG/DTA curves for the mixture $CeO_2 + BaCO_3 + 2(NH_4)_2HPO_4$.

Ce 3d spectra of Ce(III) and Ce(IV) are very different (Fig. 9), permitting to use them as a fingerprint of the Ce oxidation state. $CePO_4$ and CeO_2 were used, as reference spectra, which contain Ce(III) and Ce(IV), respectively. The "$BaCe(PO_4)_2$" sample was cleaned by mechanical abrading immediately before introduction into the spectrometer. The sample initially did not show any Ce in the surface layers, which is taken as an indication of its heterogeneity. In contrast, both reference samples (CeO_2 and $CePO_4$) were cleaned without polishing.

The shape of the Ce 3d pattern is directly related to the complex electronic structure of the Ce 4f states, i.e., to their occupation (f^1 or f^0) and their hybridisation with the O 2p levels. The associated final states therefore depend upon the oxidation state [31,32]. In particular, the peak at 920 eV is attributed to the f^0 final state that occurs only in Ce(IV). In Ce(III), this configuration does not exist (only f^1). Therefore, the absence of this peak proves that Ce in "$BaCe(PO_4)_2$" is at the oxidation state +3. The similarity between the Ce 3d spectra of "$BaCe(PO_4)_2$" and $CePO_4$ is further evidence for this.

We would like to mention that the only two Ce(IV) phosphates have been well characterised to date. The first one was obtained hydrothermally at 200 °C [33–35] and corresponded to the formula $Ce(PO_4)(HPO_4)_{0.5}(H_2O)_{0.5}$. Further thermal treatment of this phosphate at temperatures of >600 °C has lead to the reduction of Ce(IV) to Ce(III) with formation of a mixture of $CePO_4$ and CeP_3O_9. The other one is a phosphate with a tunnel structure, $K_4CeZr(PO_4)_4$, and it was obtained by a self-flux technique at 640 °C [36]. At the reaction temperature, a powder of $CePO_4$ appeared as the secondary product.

Taking into account all the evidences, we can conclude at this stage that "$BaCe(PO_4)_2$" does not form, because Ce(IV) is reduced to Ce(III) even in an oxidising atmosphere. For the same reasons, the existence of other Ce(IV) phosphates is doubtful [14,37,38]. However, additional investigations are required, since the XRD studies are not sufficient to elucidate the reaction mechanism in such compounds.

For example, a graphical analysis shows that the unit-cell volumes regularly increases for $M^{II}Th(PO_4)_2$ compounds reported in [3] as a function of the M^{II} ionic radius (Fig. 10). Conversely, the unit-cell volume of the "$M^{II}Ce(PO_4)_2$" compounds reported in [14] are indistinguishable from each other and from the volume of $CePO_4$ as calculated in [27,30].

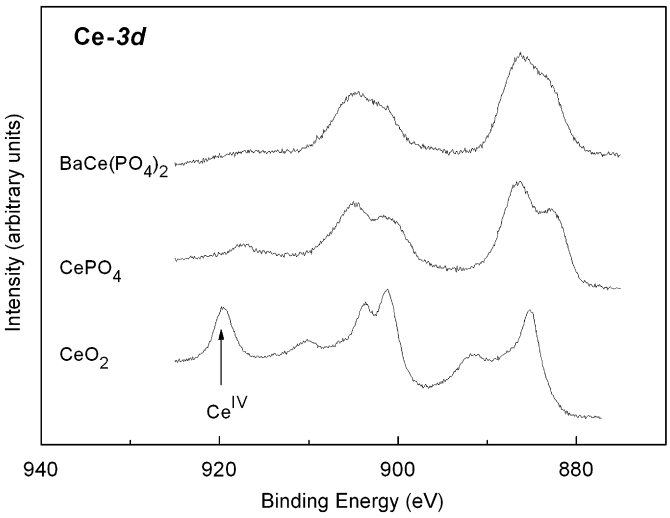

Fig. 9. XPS spectrum of "$BaCe(PO_4)_2$" in comparison with spectra from $CePO_4$ and CeO_2 reference samples.

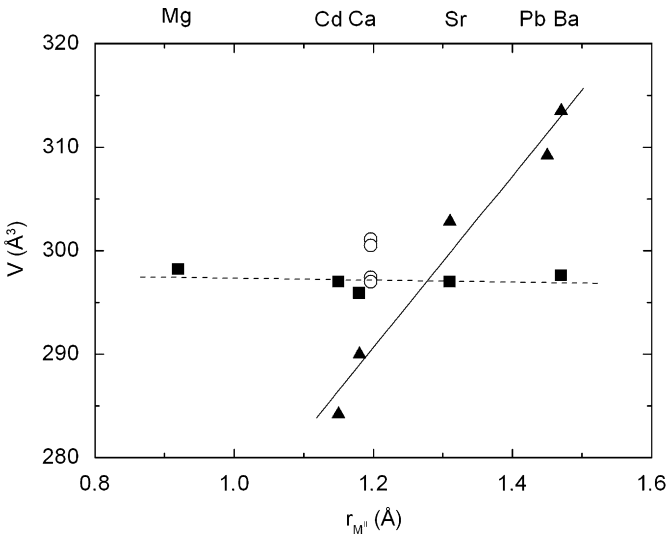

Fig. 10. Variation of the unit-cell volumes of $M^{II}Th(PO_4)_2$ and "$M^{II}Ce(PO_4)_2$" compounds as a function of the ionic radii [25] of the MIV cations. (▲), $M^{II}Th(PO_4)_2$ compounds; (■), "$M^{II}Ce(PO_4)_2$" compounds; (o), $CePO_4$ reported in different studies [27–30].

As already mentioned, $BaTh(PO_4)_2$ crystallises in the $P2_1/n$ with the lattice parameters listed in Table 1 [3]. The determined unit-cell volume fits perfectly into the trend given by the unit-cell volume of $M^{II}Th(PO_4)_2$ as a function of the ionic radii [3,39–42]. The compound reported by Brandel et al. [16], although single phase, was not indexed.

4. Phase transition in $BaM^{IV}(PO_4)_2$ compounds with yavapaiite structure

Fukuda et al. [7] discovered and characterised a first-order phase transition in $BaZr(PO_4)_2$ and measured its anisotropic thermal expansion. The phase transition occurs at approximately 460 °C and the high-temperature polymorph was indexed based on an orthorhombic unit cell.

We independently studied the phase transformation of this compound by Raman spectroscopy and drop calorimetry. Both techniques confirmed the occurrence of a phase transition near 460 °C [8,43]. However, the Raman spectrum of the high-temperature polymorph of $BaZr(PO_4)_2$ shows a decreased number of bands [43]. Group theoretical considerations have shown that the reduction of the number of Raman bands is only consistent with a trigonal structure, where the Ba and Zr atoms are located at a D_{3d} site, the P and two O at a C_{3v}, and six O atoms at a C_s site in the D_{3d} factor group. Possible space groups for this polymorph were found to be: $D^1_{3d}(P\bar{3}1m)$, $D^3_{3d}(P\bar{3}m1)$, or $D^5_{3d}(R\bar{3}m)$. To resolve this discrepancy, further spectroscopic studies were performed on $BaM^{IV}(PO_4)_2$ compounds with M^{IV} = Ti, Zr, Hf, and Sn. The frequencies of the fundamental Raman bands for $BaM^{IV}(PO_4)_2$ compounds with M^{IV} = Ti, Zr, Hf, and Sn at room temperature and 560 °C are listed in Table 4.

A phase transition was observed in $BaHf(PO_4)_2$ at about 520 °C and further characterised by thermodynamic and spectroscopic methods [10]. By analogy with $BaZr(PO_4)_2$, we concluded that the high-temperature phase of this compound has the same crystal structure as the high-temperature polymorph of $BaZr(PO_4)_2$.

Table 4
The Raman band positions of polymorphs of $BaM^{IV}(PO_4)_2$ (M^{IV} = Ti, Zr, Hf, Sn) at room and high temperature (in cm^{-1})

Vibrational modes	Lattice	PO_4 bending ($\nu_2+\nu_4$)	PO_4 stretching ($\nu_2+\nu_4$)
$BaTi(PO_4)_2$ at 25 °C	100[a], 159.5[a], 186.5[a] 226, 239, 356	430, 460, 547, 577, 642	950, 963, 1058, 1181
$BaZr(PO_4)_2$ at 25 °C	167, 209, 237, 335	417, 454, 551, 586, 645	974, 993, 1047, 1193
$BaZr(PO_4)_2$ at 560 °C	222, 229	425, 557, 604	979, 1045, 1191
$BaHf(PO_4)_2$ at 25 °C	95[a], 135, 171, 213, 244, 340	411, 460, 552, 588, 650	983, 1006, 1055, 1197
$BaHf(PO_4)_2$ at 560 °C	156, 178, 226, 293	425, 559, 605	994, 1052, 1194
$BaSn(PO_4)_2$ at 25 °C	203, 239, 356	460, 547, 577, 577, 642	950, 963, 1058, 1181

[a]Reported by Paques-Ledent [6].

Further thermogravimetric studies on $BaM^{IV}(PO_4)_2$ compounds with yavapaiite structure indicate single events during heating and cooling, which can be assigned to similar first-order phase transitions. For example, we observed a single event in the DTA curve of $BaTi(PO_4)_2$ at 956 °C (onset temperature) upon heating, while the reverse event occurs at 894 °C during cooling. Similarly, the DTA curve recorded for $BaSn(PO_4)_2$ indicates a single event at 1332 °C during heating and at 1327 °C during cooling. The thermogravimetric study on $BaGe(PO_4)_2$ did not reveal any phase transition up to 1600 °C, but it cannot be ruled out that a phase transition occurs at higher temperatures.

Unfortunately, due to experimental limitations, we could not study the evolution of the Raman spectra above 600 °C. We can just envision a similar phase transition in other $M^{II}M^{IV}(PO_4)_2$ compounds where M^{IV} = Ti, Zr, Hf, Ge, Sn, Mo and M^{II} = Ba, Ra [10].

5. Solid solutions

Several studies on the solid solutions of $BaM^{IV}(PO_4)_2$ compounds have been reported. In a study on monazite compounds proposed as nuclear waste form materials, Pepin et al. [37] reported the synthesis of $Ce^{III}_{1-2x}Ce^{IV}_{x}M^{II}_{x}PO_4$ compounds with M^{II} = Ba and Sr for $x<0.1$. For $x\geqslant 0.1$, the final powder consists in a monazite with unchanged cell parameters and alkaline earth pyrophosphate.

The substitution of Zr with Hf on the M^{IV} cation site was studied by Miao and Torardi [44]. The final solid solution with the nominal composition $BaHf_{1-x}Zr_x(PO_4)_2$ ($x\leqslant 0.2$) crystallises in the monoclinic $C2/m$ space group. The synthesis products with $x>0.2$ were not pure phases. They were characterised by minor impurities of HfP_2O_7 and/or ZrP_2O_7. In addition, the powder XRD patterns further revealed additional, unidentified diffraction lines.

Recently, Fukuda et al. [45] studied the substitution of Ba with Sr in $BaZr(PO_4)_2$, with the general formula $Sr_xBa_{1-x}Zr(PO_4)_2$. Only for $x\leqslant 0.1$ the solid solution crystallised in the monoclinic $C2/m$ space group. For $0.2\leqslant x\leqslant 0.7$, the obtained solid solution exhibited a yavapaiite superstructure along the a-axis. For $0.8\leqslant x\leqslant 0.9$, a mixture of the above-mentioned phase and a triclinic phase isostructural with the $SrZr(PO_4)_2$ end member was observed.

In a comprehensive study, Montel et al. [3] investigated the evolution of the unit-cell parameters of the $La_{2-2x}M^{II}_{x}Th_x(PO_4)_2$ solid solution series as a function of the composition. For M^{II} = Ca, Cd, Sr, and Pb, the solid solutions are continuous, but the unit-cell parameters vary linearly with composition only for Ca, Cd, and Sr. An interesting case is the one of Ba, where a miscibility gap appears for $x = 1$; for higher substitution degree, additional phases like large-cell brabantite or $ThO_2 + Ba_7Th(PO_4)_6$ can by observed by XRD analyse.

We have succesfully synthesised $Ba_xM^{IV}_{x}Ce_{2-2x}(PO_4)_2$ (M^{IV} = Zr, Hf) monazite-like compounds [46] by a solid-state reaction for $x\leqslant 0.2$ (M^{IV} = Zr) and $x\leqslant 0.1$ (M^{IV} = Hf). The low miscibility of $BaM^{IV}(PO_4)_2$ (M^{IV} = Zr, Hf) compounds in $CePO_4$ was explained on the basis of the monoclinic-to-trigonal phase transition that occurs in $BaZr(PO_4)_2$ and $BaHf(PO_4)_2$. For higher values of x, a bi- or triphasic system was obtained as a function of the substitution degree.

6. Applications to nuclear waste disposal

$BaM^{IV}(PO_4)_2$ phosphates may find practical applications in the conditioning of long-lived radionuclides. Phosphates with monazite–brabantite [18,47–55], apatite [56,57], thorium–phosphate–diphosphate [58–60], britholites [61,62], and NZP structures [63–66] have all been proposed as potential nuclear waste form materials.

Numerous geochemical studies have shown that monazite presents a high aqueous durability. Monazite can incorporate high amounts of tetravalent Th and U and has a very good radiation resistance, i.e., despite high actinide contents, natural monazite has not been reported to be metamict (amorphous) as a result of self-irradiation [67–69]. The solid-solution monazite–brabantite permits the incorporation of both trivalent and tetravalent actinides in the same compound. Also the incorporation of neutron absorbers as Gd on the M^{III} sites or Hf on the M^{IV} sites are possible, which is a pre-requested property for the sustainability of the proposed solid solutions as a nuclear waste form.

The present review has shown that $BaM^{IV}(PO_4)_2$ compounds containing a tetravalent cation with an ionic radius smaller than 0.72 Å (into the coordination VI) crystallise in the monoclinic $C2/m$ space group and not in the $P2_1/n$. This yavapaiite structure is not stable during heating and transforms to a trigonal modification. However, we have demonstrated that $BaZr(PO_4)_2$ and $BaHf(PO_4)_2$ show a limited solubility in $CePO_4$ [46], the structure being of the monazite type—a phase which could be a ceramic waste form for actinides. The Hf incorporation is two orders of magnitude higher than the one previously reported [70]. This finding increases the ranking of monazites to "high" in terms of chemical flexibility [71].

$BaM^{IV}(PO_4)_2$ compounds containing a tetravalent cation with a larger ionic radius, crystallise in the monazite structure. A clear case is $BaTh(PO_4)_2$ [3]. The case of the other actinides as well as cerium, which are also expected to crystallise in the $P2_1/n$ space group, is complicated by the possibility of multiple stable valence states. We have clearly demonstrated that cerium is present as Ce(III) in these compounds, and cannot be stabilised as Ce(IV). Similarly our experience has shown that Pu(IV) can partially reduce to Pu(III) [55]. Also our attempts to synthesise $BaU(PO_4)_2$ were not successful, evidently because of the high stability of UP_2O_7. On the basis of these observations, we conclude

that the existence of $BaPu(PO_4)_2$ as a pure compound is doubtful.

Acknowledgments

K.P. and D.B. acknowledge the European Commission for support given in the frame of the programme "Training and Mobility of Researchers". The authors thank Mr. B. Cremer and Dr. C.C. Pavel for the microscopic characterisation of the samples.

References

[1] V. Brandel, N. Dacheux, J. Solid State Chem. 177 (2004) 4743.
[2] V. Brandel, N. Dacheux, J. Solid State Chem. 177 (2004) 4755.
[3] J.M. Montel, J.L. Devidal, D. Avignant, Chem. Geol. 191 (2002) 89.
[4] I.V. Tananev (Ed.), The Chemistry of Tetravalent Elements Phosphates, Nauka, Moskow, 1972.
[5] R. Masse, A. Durif, C.R. Acad. Sci. Paris C 274 (1972) 1692.
[6] M.T. Paques-Ledent, J. Inorg. Nucl. Chem. 39 (1977) 11.
[7] K. Fukuda, A. Moriyama, T. Iwata, J. Solid State Chem. 178 (2005) 2144.
[8] K. Popa, R.J.M. Konings, P. Boulet, D. Bouëxière, A.F. Popa, Thermochim. Acta 436 (2005) 51.
[9] V.I. Petkov, A.I. Orlova, J. Therm. Anal. 54 (1998) 71.
[10] K. Popa, R.J.M. Konings, O. Beneš, T. Geisler, A.F. Popa, Thermochim. Acta 451 (2006) 1.
[11] K. Popa, R.J.M. Konings, D. Bouëxière, A.F. Popa, T. Geisler, Adv. Sci. Technol. 45 (2006) 2012.
[12] R.A. McCauley, F.A. Hummel, Trans. Br. Ceram. Soc. 67 (1968) 624.
[13] A. Leclaire, M.M. Borel, J. Chardon, B. Raveau, J. Sol. State Chem. 116 (1995) 364.
[14] A.I. Orlova, D.B. Kitaev, N.G. Kazantzev, S.G. Samoilov, V.S. Kurazhkovskaya, E.N. Vopilina, Radiochemistry 44 (2002) 326.
[15] W.C. Luth, C.O. Ingamels, Am. Miner. 48 (1963) 255.
[16] V. Brandel, N. Dacheux, J. Rousselle, M. Genet, C.R. Chim. 5 (2002) 599.
[17] M.A. Colani, C.R. Chim. (1909) 59.
[18] C.E. Bamberger, R.G. Haire, G.M. Begun, L.C. Ellingboe, Inorg. Chim. Acta 94 (1984) 49.
[19] C.E. Bamberger, in: A.J. Freeman, C. Keller (Eds.), Handbook on the Physics and Chemistry of the Actinides, vol. III, North-Holland, Amsterdam, 1985, pp. 294–304.
[20] V. Brandel, N. Dacheux, M. Genet, J. Sol. State Chem. 121 (1996) 467.
[21] D.A. Woodcock, P. Lightfood, R.I. Smith, J. Mater. Chem. 9 (1999) 2631.
[22] E.R. Gobechiya, Y.U.K. Kabalov, V.I. Petkov, M.V. Sukhanov, Crystallogr. Rep. 49 (2004) 741.
[23] D. Krabbenhoft, McCarthy, ICDD Grant-in-Aid (1981) JC-PDS File no. 033-0180.
[24] L. Keller, McCarthy, ICDD Grant-in-Aid, JCPDS File no. 33-150, North Dakota State University, Fargo, North Dakota, USA, 1982.
[25] R.D. Shannon, Acta Crystallogr. A 32 (1976) 751.
[26] E.J. Graeber, A. Rosenzweig, Am. Miner. 56 (1971) 1917.
[27] G.W. Beall, L.A. Boatner, D.F. Mullica, W.O. Milligan, J. Inorg. Nucl. Chem. 43 (1981) 101.
[28] J.G. Pepin, E.R. Vance, J. Inorg. Nucl. Chem. 43 (1981) 2807.
[29] Y. Ni, J.M. Hughes, A.N. Mariano, Am. Miner. 80 (1995) 21.
[30] C. Thiriet, R.J.M. Konings, P. Javorský, F. Wastin, Phys. Chem. Miner. 31 (2004) 1.
[31] M. Romeo, K. Bak, J. El Fallah, F. Le Normand, L. Hilaire, Surf. Interface Anal. 20 (1993) 508.
[32] B. Glorieux, R. Berjoan, M. Matecki, A. Kammouni, D. Perarnau, Appl. Surf. Sci. 253 (2007) 3349.
[33] V. Brandel, N. Clavier, N. Dacheux, J. Solid State Chem. 178 (2005) 1054.
[34] M. Nazaraly, G. Wallez, C. Chanéac, E. Tronc, F. Ribot, M. Quarton, J.P. Jolivet, Angew. Chem. Int. Ed. 44 (2005) 5691.
[35] M. Nazaraly, G. Wallez, C. Chanéac, E. Tronc, F. Ribot, M. Quarton, J.P. Jolivet, J. Phys. Chem. Solids 67 (2006) 1075.
[36] I.V. Ogorodnyk, I.V. Zatovsky, V.N. Baumer, N.S. Slobodyanik, O.V. Shishkin, Acta Crystallogr. C 62 (2006) i100.
[37] J.G. Pepin, E.R. Vance, G.J. McCarthy, Mater. Res. Bull. 16 (1981) 627.
[38] A.I. Orlova, M.L. Spiridonova, M.P. Orlova, I.V. Pet'kov, Y.K. Kabalov, N.V. Zubkova, I.A. Kulikov, G.N. Kazantsev, S.G. Samoilov, Russ. J. Inorg. Chem. 49 (2004) 1331.
[39] H. Schwarz, Z. Annorg. Allg. Chem. 3-4 (1964) 175.
[40] Y. Hikichi, K. Hukuo, J. Shiokawa, Nihon-Kagakki-shi (J. Chem. Soc. Japan) 12 (1978) 1635 (in Japanise).
[41] D. Rose, N. Jb. Miner. Mh. 6 (1980) 247.
[42] R. Podor, M. Cuney, Am. Miner. 82 (1997) 765.
[43] T. Geisler, K. Popa, R.J.M. Konings, A.F. Popa, J. Solid State Chem. 179 (2006) 1490.
[44] C.R. Miao, C.C. Torardi, J. Solid State Chem. 155 (2000) 229.
[45] K. Fukuda, T. Iwata, A. Moriyama, S. Hashimoto, J. Solid State Chem. 179 (2006) 3870.
[46] K. Popa, H. Leiste, T. Wiss, R.J.M. Konings, J. Radioanal. Nucl. Chem. 273 (2007) 563.
[47] G.J. McCarthy, W.B. White, D.E. Pfoertsch, Mater. Res. Bull. 13 (1978) 1239.
[48] B.C. Sales, C.W. White, L.A. Boatner, Nucl. Chem. Waste Manage. 4 (1983) 281.
[49] A. Tabuteau, M. Pagès, J. Livet, C. Musikas, J. Mater. Sci. Lett. 7 (1988) 1315.
[50] L.A. Boatner, B.C. Sales. in: W. Lutze, R.C. Ewing, (Eds.), Radioactive Waste Forms For the Future, 1998, p. 495–561.
[51] B.E. Burakov, M.A. Yagovkina, V.M. Garbuzov, A.A. Kitsay, V.A. Zirlin, Mater. Res. Symp. Proc. 824 (2004) 219.
[52] N. Dacheux, N. Clavier, A.C. Robbison, O. Terra, F. Audubert, J.E. Lartigue, C. Guy, C.R. Chim. 7 (2004) 1141.
[53] X. Deschanels, V. Picot, B. Glorieux, F. Jorion, S. Peuget, D. Roudil, C. Jégou, V. Broudic, J.N. Cachia, T. Advocat, C. Den Auwer, C. Fillet, J.P. Coutures, C. Hennig, A. Scheinost, J. Nucl. Mater. 352 (2006) 233.
[54] J.M. Montel, B. Glorieux, A.M. Seydoux-Guillaume, R. Wirth, J. Phys. Chem. Solids 67 (2006) 2489.
[55] D. Bregiroux, R. Belin, P. Valenza, F. Audubert, D. Bernache-Assollant, J. Nucl. Mater. 366 (2007) 52.
[56] W.J. Weber, R.C. Ewing, A. Meldrum, J. Nucl. Mater. 250 (1997) 147.
[57] R.C. Moore, K. Holt, H. Zhao, A. Hasan, N. Awwad, M. Gasser, C. Sanchez, Radiochim. Acta 91 (2003) 721.
[58] N. Dacheux, R. Podor, B. Chassigneaux, V. Brandel, M. Genet, J. Alloys Compd. 271–273 (1998) 236.
[59] O. Terra, N. Dacheux, F. Audubert, R. Podor, J. Nucl. Mater. 352 (2006) 224.
[60] C. Tamain, N. Dacheux, F. Garrido, A. Habert, N. Barré, A. Özgümüs, L. Thomé, J. Nucl. Mater. 358 (2006) 190.
[61] D. Bregiroux, F. Audubert, E. Champion, D. Bernache-Assollant, Matter. Lett. 57 (2003) 3526.
[62] O. Terra, F. Audubert, N. Dacheux, C. Guy, R. Podor, J. Nucl. Mater. 366 (2007) 70.
[63] R. Roy, E.R. Vance, J. Alamo, Matter. Res. Bull. (1982) 585.
[64] B.E. Scheetz, D.K. Agrawal, E. Breval, R. Roy, Waste Manage. 14 (1994) 489.
[65] M.P. Orlova, A.I. Orlova, E.R. Gobechiya, Y.K. Kabalov, G.I. Dorokhova, Crystallogr. Rep. 50 (2005) 55.
[66] D.M. Bykov, E.R. Gobechiya, Y.U.K. Kabalov, A.I. Orlova, S.V. Tomilin, J. Solid State Chem. 179 (2006) 3101.

[67] W.J. Weber, R.C. Ewing, C.R.A. Catlow, T. Diaz de la Rubia, L.W. Hobbs, C. Kinoshita, H. Matzke, A.T. Motta, M. Nastasi, E.K.H. Salje, E.R. Vance, S.J. Zinkle, J. Mater. Res. 13 (1998) 1434.
[68] C. Guy, F. Audubert, J.E. Lartigue, C. Latrille, T. Advocat, C. Fillet, C.R. Phys. 3 (2002) 827.
[69] B. Glorieux, M. Matecki, F. Fayon, J.P. Coutures, S. Palau, A. Douy, G. Peraudeau, J. Nucl. Mater. 326 (2004) 156.
[70] P.E.D. Morgan, R.M. Housley, J.B. Davis, M.L. DeHaan, Final Technical Report Contract No. DE-FG07-96ER45617, Rockwell Scientific, Camino Dos Rios, Thousand Oaks, CA, USA.
[71] G. Lumpkin, Elements 2 (2006) 365.